ISSN 2706-655X Vol.3, Issue 5: 10-16, DOI: 10.25236/IJFET.2021.030502

Research on Dangerous Points of Local Wall-Thinning Penstock

Yang Zhang[1,2*]

[1]*China Institute of Water Resources and Hydropower Research, Beijing 100038, China*
[2]*School of Water Consenvancy and Ecological Engineering, Nanchang Institute of Technology, Nanchang 330099, China*
[*]*Corresponding author*

Abstract: *This paper is aimed at studying the method of predicting dangerous points of local wall-thinning penstock. To begin with, the proposed failure analysis method was proved to be reliable in combination with test results. Next, the volume ratio of the plastic zone when the pipes with local wall-thinning and pipes without defect are failed was regarded as the quantitative index of failure mode. Based on this, the corresponding relationship between the penstock failure mode and the geometric parameters of local wall-thinning was established. Moreover, the corresponding relationship between geometric parameters of local wall-thinning and the positions of dangerous point was disclosed in accordance with the equivalent stress distribution when the local wall-thinning penstock fails. According to the results, main dangerous points can be found near the axial boundary and the local wall-thinning center of local wall-thinning penstock.*

Keywords: *Penstock, Local thinned defect, Dangerous point*

1. Introduction

Local wall-thinning phenomenon can be frequently found at the wall of the penstock that bears minute rough granules carried by high-pressure water under the corrosive effect of external materials, leading to reduction in bearing capacity, fatigue crack initiation, and local expansion, etc. Hence, it is essential for predicting dangerous points for local wall-thinning penstock in hydropower station.

In most cases, dangerous points for failure, as the most vulnerable parts of pipes with local wall-thinning, might trigger perforation, cracking and explosion of the pipe. For this reason, accurately predicting dangerous points can contribute to the safe operation of pipes. Mondal [1, 2] suggested that dangerous points might occur at different positions upon studying two groups of local wall-thinning pipes with different thinning parameters, successively. Also, Fan X Y [3] indicated that dangerous points of local wall-thinning pipe are found at the axial boundary of local wall-thinning. Ma X [4] believed that the position of the dangerous point is significantly affected by thinning parameters inside the pipe. These researches have showed that local wall-thinning parameters have an impact on the position of the dangerous point on the pipe. But current researches have rarely presented methods of predicting the dangerous points.

Given this, this paper carried out a study on the dangerous points of local wall-thinning penstock. Specifically, the volume ratio of the plastic zone when the pipes with local wall-thinning and pipes without defect are failed was regarded as the quantitative index of failure mode. Then, positions of dangerous points on the penstock were determined by the equivalent stress distribution when the local wall-thinning penstock fails. On this basis, the method of predicting dangerous points on the local wall-thinning penstock was established.

2. Analysis Method and Verification of Local Wall-Thinning Penstock Failure Mechanism

2.1. Determination of Failure Mechanism

The failure mechanism of local wall-thinning penstocks was studied using EPIA (Elastic-plastic Incremental Analysis) to determine the relational expression for judging the dangerous points of the penstock. The volume ratios of the plastic zone when local wall-thinning penstock fails and when the

ISSN 2706-655X Vol.3, Issue 5: 10-16, DOI: 10.25236/IJFET.2021.030502

corresponding zero-defect pipeline fails were used as the quantification index of failure mode. Eq. (1) and Eq. (2) were adopted to judge the failure mode type of the local wall-thinning penstock:

$$\text{Global Failure}: \ V_L / V \geq 60\% \tag{1}$$

$$\text{Local Failure}: \ V_L / V \leq 20\% \tag{2}$$

where, V_L is the volume of the plastic zone when the local wall-thinning penstock fails, and V is the volume of the plastic zone when the zero-defect penstock fails.

The position of the dangerous point when the penstock fails is determined by Eq. (3):

$$\sigma_d = \max\left\{\sigma^i{}_{\text{Mises}}\right\}, \quad i = 1, 2, \ldots N \tag{3}$$

where, σ_d is the Von Mises stress at the dangerous point on the penstock; $\sigma^i{}_{\text{Mises}}$ is the Von Mises stress at the ith node; and N is the total number of nodes.

2.2. Verification of the Analysis Method

2.2.1. Benjamin explosion test

The IDTS2 specimen used by the Benjamin [5] test was selected. The penstock was made of API X80 steel with the yield strength and tensile strength as 534.1MPa and 713.8MPa, respectively. The elastic modulus was 2.0×105MPa, and the Poisson's ratio was 0.3. The ultimate bearing capacity obtained by EPIA is shown in Table 1. And the failure mode and stress distribution when the penstock fails are presented in Fig. 1.

Table 1 Ultimate bearing capacity of IDTS2 specimen used by the Benjamin test

Specimen	2A/mm	2B/mm	C/mm	Test result[5]/MPa	Result obtained in this paper/MPa	Error/%
IDTS2	39.60	31.90	5.39	22.68	22.00	3.18

According to Table 1, the calculation results of the ultimate bearing capacity show good agreement with the test results, presenting an error of 3.18%. More than that, the maximum stresses of all calculation methods are found at the near non-thinning area where is parallel to the penstock axis, which is consistent with the failure area and mode of the test. The study discloses that the failure area is confined to a small range of the thinning area, and the dangerous point occurs near the non-thinning area where is parallel to the axis.

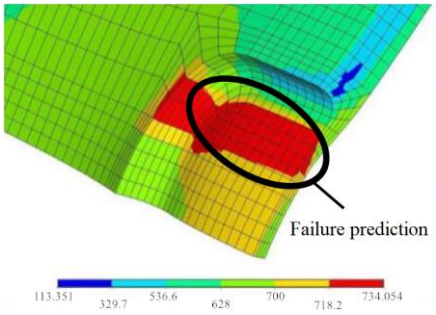

(a) Stress distribution calculated by Benjamin [5]

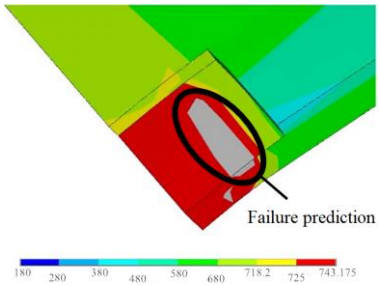

(b) Stress distribution obtained in this paper

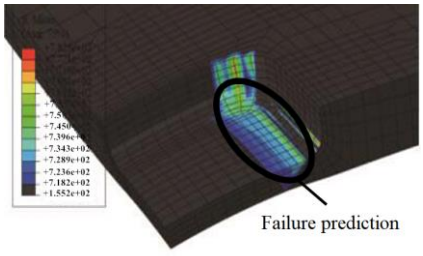

(b) Stress distribution calculated in reference [6]

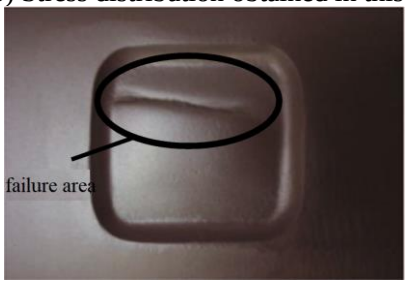

(d) dangerous points of IDTS2 specimen

Figure. 1 Stress distribution and dangerous points of IDTS2 specimen

ISSN 2706-655X Vol.3, Issue 5: 10-16, DOI: 10.25236/IJFET.2021.030502

3. Calculation Model and Parameters of Local Wall-Thinning Penstock

A local wall-thinning penstock buried in the anchorage block at both ends is presented in Fig. 2. The span is L; the outer radius Ro is 1.5m; the inner radius Ri is 1.48m; and the wall thickness t is 20mm. Local wall-thinning parameters are thinning axial length 2A, thinning circumferential length 2B (corresponding to 2θ) and thinning depth C. The penstock is made of Q345D steel, and its true stress-strain curve [12] is shown in Fig. 3, with the yield strength of 345MPa, the elastic modulus of 2.06×105MPa, and the Poisson's ratio of 0.3. Besides, structural modeling and analysis were performed using the ANSYS finite element software. The penstock wall was simulated with 20-node SOLID95 elements. Meanwhile, the local wall-thinning area was simulated with the groove-shaped pit. Based on this, a finite element calculation model was established through taking a quarter of the penstock section in accordance with the symmetries of structure and load, as shown in Fg.4. In this way, it can divide the wall of the zero-defect area into 4 layers of elements along the thickness direction, divide the area with local wall-thinning into 2 layers of elements, and finely divide the elements along the axial and circumferential directions on the thinning section. In addition, symmetrical constraints were imposed on the symmetric plane, and fixed constraints were imposed on both ends of the penstock section with considerations in the effect of uniform internal pressure and water weight.

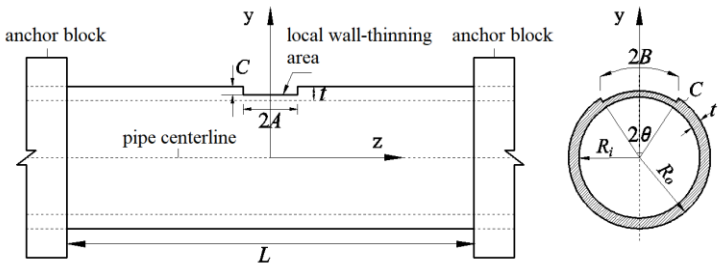

Figure. 2 Local wall-thinning penstock

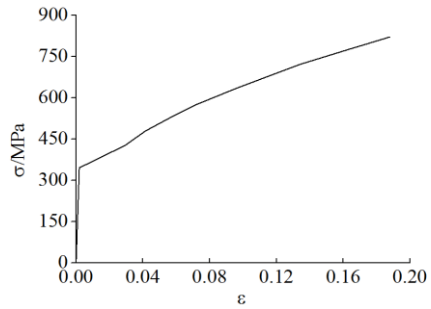

Figure. 3 Stress-strain relationship of Q345D

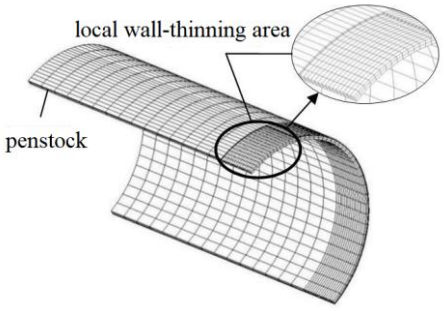

Figure. 4 Finite element mesh of local wall-thinning penstock

To facilitate the analysis below, some of shape parameters and local wall-thinning parameters of the penstock are nondimensionalized:

$$l = L / 2R_o; \quad a = A / \sqrt{R_o t}; \quad b = B / \pi R_o; \quad c = C / t \tag{4}$$

ISSN 2706-655X Vol.3, Issue 5: 10-16, DOI: 10.25236/IJFET.2021.030502

where, l is the nondimensionalized pipe span; a, b and c are nondimensionalized local wall-thinning axial half-length, local wall-thinning circumferential half-length and local wall-thinning depth, respectively.

4. Prediction of Dangerous Points on the Local Wall-Thinning Penstock

To predict the position of the dangerous point when the local wall-thinning penstock fails, the stress distribution was studied for five characteristic points of the A to E calculation models shown in Fig. 5. Note that LAC=5m.

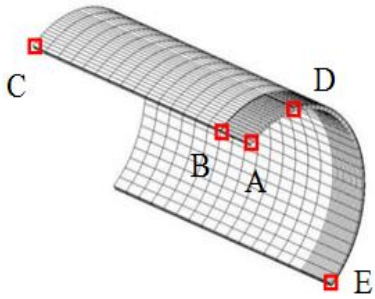

Figure. 5 Selection of dangerous points of local thinning pressure steel pipe

4.1. Influence of Wall-Thinning Axial Length a on the Dangerous Point of Local Wall-Thinning Penstock

To reveal the influence law of the local wall-thinning axial length a on the dangerous point of the local wall-thinning penstock, the following nondimensionalized local wall-thinning geometric parameter calculation schemes are taken, including a=0.6, 1.0, 3.0, 4.0, 5.0, 6.0, 7.0, 8.0, 9.0, 10.0, b=0.2, c=0.5, σ_{Mises} stress distributions along the axial and circumferential directions of all schemes are shown in Fig 7.

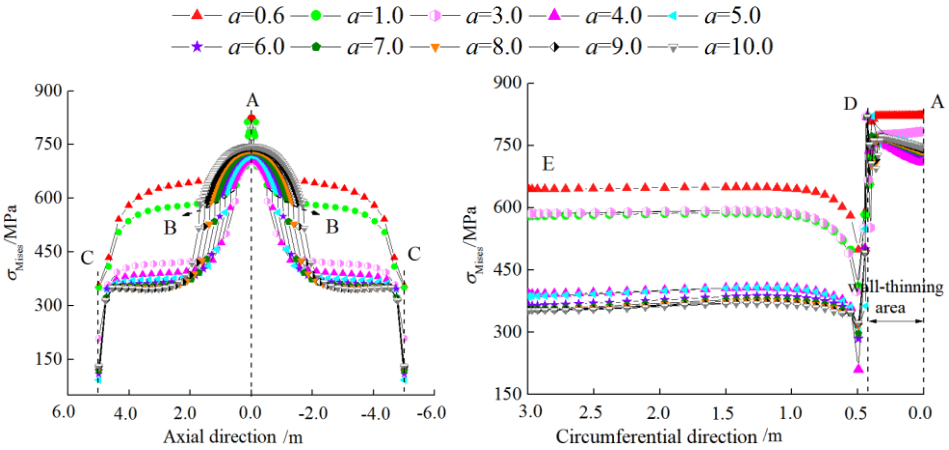

(a) Axial direction Circumferential direction

Figure. 6 Influence law of wall-thinning axial length a on σ_{Mises} stress distribution

As can be seen from Fig. 6(a), σ_{Mises} at point A is the largest, followed by point B and point C under the influence of varied nondimensionalized thinning axial length a. With the change of a, the variations of the σ_{Mises} curve along the axial distribution are similar, presenting a trend of first decreasing with the rising distance away from point A and then decreasing further after it becomes stable. As can be observed from Fig. 6(b), the maximum σ_{Mises} of the penstock is distributed in the local wall-thinning area under the influence of varied nondimensionalized thinning axial length a. More precisely, when $a \le 0.6$, the maximum σ_{Mises} can be found near point A and point D; when $a > 0.6$, the maximum σ_{Mises} can be found only near point D. Evidently, the nondimensionalized

ISSN 2706-655X Vol.3, Issue 5: 10-16, DOI: 10.25236/IJFET.2021.030502

thinning axial length a has a remarkable influence on the position of the dangerous point of the penstock. Hence, the influence of the parameter a should be considered in the prediction of the dangerous point of the penstock.

4.2. Influence of Thinning Circumferential Length b On The Dangerous Points Of The Local Wall-Thinning Penstock

To reveal the influence law of the local wall-thinning circumferential length b on the dangerous point of the local wall-thinning penstock, the following nondimensionalized local wall-thinning geometric parameter calculation schemes are taken, including a=5.0, b=0.08, 0.10, 0.20, 0.30, 0.50 and 0.60, c=0.5, σ_{Mises} stress distributions along the axial and circumferential directions of all schemes are shown in Fig. 7.

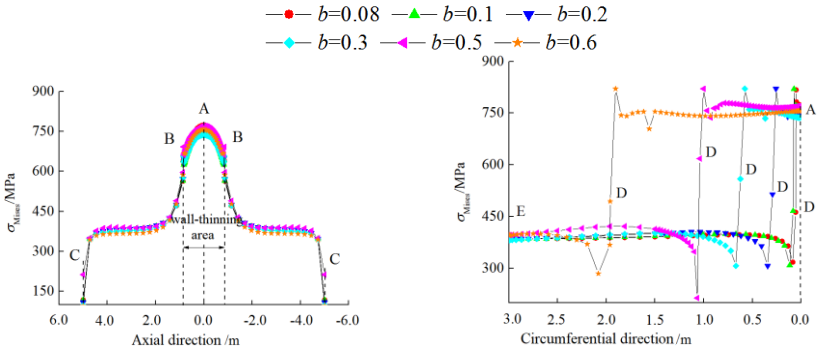

(a) Axial direction (b) Circumferential direction

Fig. 7 Influence law of thinning circumferential length b on σ_{Mises} *stress distribution*

As can be seen from Fig. 7(a), σ_{Mises} at point A is the largest, followed by point B and point C under the influence of varied nondimensionalized thinning circumferential length *b*. With the change of *b*, the variations of the σ_{Mises} curve along the axial distribution are consistent, presenting a trend of first decreasing with the rising distance away from point A and then decreasing further after it becomes stable. As can be observed from Fig. 7(b), the maximum σ_{Mises} can be witnessed only inside the local wall-thinning section near point D, no matter what *b* is taken. Based on the analysis, the thinning circumferential length *b* has no impact on the position of the dangerous point. In other words, the influence of parameter *b* on the dangerous point of the penstock can be ignored.

4.3. Influence of Thinning Depth c on the Dangerous Points of Local Wall-Thinning Penstock

To reveal the influence law of the local wall-thinning depth *c* on the dangerous point of the local wall-thinning penstock, the following nondimensionalized local wall-thinning geometric parameter calculation schemes are taken, including a=5.0, b=0.2, c=0.3, 0.4, 0.5, 0.6, 0.7 and 0.8. σ_{Mises} stress distributions along the axial and circumferential directions of all schemes are shown in Fig. 8.

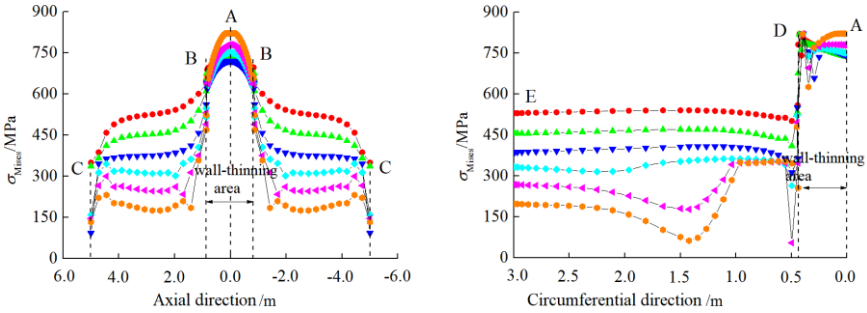

(a) Axial direction (b) Circumferential direction

Figure. 8 Influence law of thinning depth c on σ_{Mises} *stress distribution*

ISSN 2706-655X Vol.3, Issue 5: 10-16, DOI: 10.25236/IJFET.2021.030502

As can be seen from Fig. 8(a), σ_{Mises} at point A is the largest, followed by point B and point C as the nondimensionalized thinning depth *c* changes. With the change of *c*, the variations of the σ_{Mises} curve along the axial distribution are similar, presenting a trend of first decreasing with the rising distance away from point A and then decreasing further after it becomes stable. As can be observed from Fig. 8(b), the maximum σ_{Mises} of the penstock is distributed in the local wall-thinning area under the influence of varied nondimensionalized thinning depth *c*. Concretely, when $c \le 0.7$, the maximum σ_{Mises} can be found in the local wall-thinning area near point D; when *c*>0.7, the maximum σ_{Mises} can be found simultaneously in the local wall-thinning areas near point A and point D. Based on the above analysis, the position of the dangerous point is markedly affected by the thinning depth *c*. Thus, the influence of the parameter *c* should be considered in the prediction of the dangerous point of the penstock.

Based on the above conclusions, the corresponding relationship between local wall-thinning parameters and dangerous points is summarized, as shown in Table 2:

Table 2 Corresponding relationship between local wall-thinning parameters and dangerous points

Thinning depth c	Wall-thinning axial length a	Dangerous points
$c \le 0.7$	$a > 0.6$	near point D
$c \le 0.7$	$a \le 0.6$	point A and near point D
$c > 0.7$	—	point A and near point D

Combining Fig. 6, Fig. 7, Fig. 8, and Table 2, it is apparent that dangerous points can be witnessed in the thinning area near point D when the local wall-thinning penstock fails and might be observed in the thinning area near point A point and point D at the same time. The study suggests that defects and carrying capacities of local wall-thinning penstock at point A and near point D should be emphasized to safeguard the safe operation of the service penstock. Hence, timely repair and reinforcement are required to prevent penstock failures incurred by dangerous points.

5. Prediction of failed penstock with local wall-thinning

To verify the reliable prediction of the dangerous point of wall-thinning penstock, the predicted results obtained in this paper were compared with the existing test results. Based on Table 3, the proposed method is proved to be reliable in determining the position of dangerous stress, which can provide a reference for safety assessment of the local wall-thinning penstock.

Table 3 Failure point prediction of the local wall-thinning penstock

Test	pipeline material	Ro/mm	2A/mm	C/mm	T/mm	a	c	Failure mode	Test result[7]	Predicted result obtained in this paper
1	X52	381.0	224.0	7.75	9.58	1.85	0.81	leakage	leakage	point A and near point D
2	X52	381.0	312.4	4.77	9.52	2.59	0.50	blast	blast	near point D
3	X52	381.0	219.2	5.99	9.80	1.79	0.61	blast	leakage	near point D
4	X60C	381.0	152.4	4.52	9.47	1.27	0.48	blast	blast	near point D
5	X60V	457.2	139.7	8.66	11.30	0.97	0.77	leakage	leakage	point A and near point D
6	X60V	457.2	121.9	7.54	9.98	0.90	0.76	leakage	leakage	point A and near point D
7	X60	533.4	165.1	6.50	10.26	1.12	0.63	blast	leakage	near point D

6. Conclusion

Based on the study on predicting the positions of failure points on the local wall-thinning penstock, it can be concluded that:

(i) Dangerous points of failed penstock with local wall-thinning occur frequently at the thinning area near the axial boundary, which might simultaneously present near the local wall-thinning center

ISSN 2706-655X Vol.3, Issue 5: 10-16, DOI: 10.25236/IJFET.2021.030502

and the local wall-thinning axial boundary. The correspondence relationships between the position of the dangerous point and two key parameters are also given.

(ii) Parameters, strength, and deformation of the penstock near the local wall-thinning center and the local wall-thinning axial boundary should be highly concerned for ensuring the safe operation of service penstocks.

References

[1] B.C. Mondal, A.S. Dhar (2017). Finite-element evaluation of burst pressure models for corroded pipelines. Journal of Pressure Vessel Technology, vol.139, no.2, p21-28.
[2] B.C. Mondal, A.S. Dhar (2015). Corrosion effects on the strength of steel pipes using FEA. Proceedings of the ASME 34th International Conference on Ocean, p1-7.
[3] X.Y. Fan, Y. Dan, Y. Gao (2016). Evaluation on local equivalent stress and plastic deformation for natural gas pipeline. Journal of Safety Science and Technology, vol.12, no.8, p136-138. (In Chinese)
[4] X. Ma, J. Li, T. Xue (2018). Study on stress and strain of pressure pipe with inner corrosion depression. Journal of Plasticity Engineering, vol.25, no.3, p268-273. (In Chinese)
[5] A.C. Benjamin, J.L.F. Freire, R.D. Vieira (2005). Burst tests on pipeline containing interacting corrosion defects. Proceedings of OMAE2005 24th international conference on offshore mechanics and arctic engineering, p403-417.
[6] X. Li, Y. Bai, C. Su (2016). Effect of interaction between corrosion defects on failure pressure of thin wall steel pipeline. International Journal of Pressure Vessels and Piping, vol.138, p8-18.
[7] J.F. Kiefner, W.A. Maxey, R.J. Eiber (1973). Failure stress levels of flaws in pressurized cylinders. Astm Special Technical Publication, vol.536, p461-481.